- Technical Paper -

ASSESSMENT OF STRENGTHENING EFFECT ON RC BEAMS WITH UHP-SHCC

Ahmed KAMAL[*1], Minoru KUNIEDA[*2], Naoshi UEDA[*3] and Hikaru NAKAMURA[*4]

ABSTRACT

Ultra High Performance Strain Hardening Cementitious Composites (UHP-SHCC) is a new strain hardening composite with outstanding mechanical and protective performance. In this study, UHP-SHCC was applied to RC beams as a tensile strengthening material, and the beams were tested under four-point bending setup. It was clarified that strengthening by UHP-SHCCs significantly contributed to increasing the load carrying capacity. And stress-strain relation obtained from the tensile tests can well simulate the response of the strengthened beams.

Keywords: UHP-SHCC, strengthening effect, load carrying capacity, deformation capacity

1. INTRODUCTION

In the last decade, fiber reinforced cementitious composites with higher ductility such as Strain Hardening Cementitious Composites (SHCC) have been developed. These new kind of materials are very effective in transferring the stress across a crack, and also provide multiple cracking and strain hardening behavior in tension. Several researches have been carried out using SHCC as a structural material instead of the ordinary concrete. For examples, Kanda et al.[1] applied SHCC to the production of shear resistant structural elements. Fukuyama et al. [2] tested SHCC elements under seismic loading.

An application on strengthening or repairing using SHCC is one of the attractive ones. For examples, Horii et al.[4], Li[5], and Li et al.[6] tried to apply SHCC to repair or retrofit of concrete structures, and confirmed the effect of the ductility of repair materials on the structural performance. Shin et al. [7] also investigated the strengthening effect of ductile fiber reinforced cementitious composite (DFRCC) that was applied to plain concrete beams. Most researches on strengthening using SHCC revealed that load carrying capacity of SHCC itself provided additional load carrying capacity to strengthened structures. Kunieda et al. [8] developed Ultra High Performance Strain Hardening Cementitious Composites (UHP-SHCC) with ultra high strength and strain hardening in tension. Especially, tensile strength of UHP-SHCC is significantly larger (twice or more) than that of ordinary SHCC. So, UHP-SHCC might be one of the effective materials for strengthening of concrete structures.

In this paper, the strengthening effect of RC beams with UHP-SHCC in tension side was assessed through four-point bending tests. The results were compared with beams strengthened by ordinary reinforced concrete (RC). In addition, analysis to predict moment-curvature relations was carried out and compared with the experimental results.

2. EXPERIMENTAL PROGRAMS

2.1 Materials

(1) Ordinary concrete for substrate beams

Table 1 shows the mix proportions of the concrete used for substrate beams. Water to cement ratio was 0.57. By conducting compressive tests on 6 cylindrical specimens with the size of ø100x200mm, the averaged compressive strength at the age of 28days, which was the date on casting of strengthening layer, was 22.7MPa. The compressive strength of the concrete at the age of 56days, which was the date on loading tests of strengthened beams, was 24MPa.

(2) Strengthening material

UHP-SHCC was used as a strengthening material in this study. Table 1 shows the mix proportions of UHP-SHCC. Water to binder ratio (W/B) was 0.22. Low heat Portland cement (density: 3.14g/cm^3) was used, and 15% of the cement content was substituted for a silica fume (density: 2.2g/cm^3). The quartz sand (less than 0.5mm in diameter, density: 2.68g/cm^3) was used as the fine aggregate. High strength polyethylene (PE) fiber was chosen for UHP-SHCC and the fiber volume in the mix was 1.5%. The diameter and length of the PE fibers were 0.012mm and 6mm, respectively. Superplasticizer was used to enhance the workability of the matrixes. Uniaxial tensile tests were conducted by using 6 dumbbell-shaped specimens (tested cross section: 10x30mm) for UHP-SHCC. Fig.1 illustrates the stress-strain relationship for the tensile tests. The averaged tensile strength and strain at the tensile

*1 Doctoral student, Department of Civil Engineering, Nagoya University, JCI Member
*2 Associate Professor, Department of Civil Engineering, Nagoya University, Dr. E., JCI Member
*3 Assistant Professor, Department of Civil Engineering, Nagoya University, JCI Member
*4 Professor, Department of Civil Engineering, Nagoya University, Dr. E., JCI Member

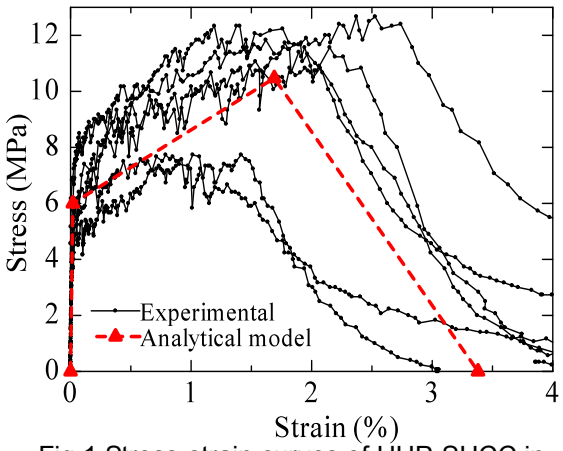

Fig.1 Stress-strain curves of UHP-SHCC in uniaxial tensile test

strength of the UHP-SHCC at the age of 28days were 10.5MPa and 1.7%, respectively. For compressive properties, 5 cylindrical specimens having the size of ø50x100mm were tested at the age of 28days. The averaged compressive strength was 86.7MPa.

For comparison, ordinary reinforced concrete was placed as a strengthening material. Table 1 shows the mix proportions of the concrete used for the strengthening layer. The averaged compressive strength of the concrete at the age of 28days, which was the date on loading tests of strengthening beams, was 20.6MPa. Two or three rebars were placed in the RC strengthening layer. D10 (SD295A, fy=362N/mm^2) and D13 (SD295A, fy=362N/mm^2) were used.

2.2 Specimens and test setup

Fourteen reinforced concrete (RC) beams with length of 1800mm and cross section of 150 x 200mm were prepared using substrate concrete shown in Table 1. Two rebars of D10 (SD295A, fy=362N/mm^2) were used as reinforcement of each beam. Stirrups of D6 (SD295) were used in the shear span at the interval of

Table 2 Type of strengthening layers

Strengthening layer	Thickness t= (mm)	Reinforcement	Reinforcement ratio in strengthening layer (%)	No. of tested beams
Non. (control beam)	0	---	---	2
UHP-SHCC	30	---	---	2
	50	---	---	2
	70	---	---	2
Reinforced concrete	70	2 D10 (SD295A)	1.36	2
	70	3 D10 (SD295A)	2.04	2
	70	3 D13 (SD295A)	3.62	2

90mm, as shown in Fig. 2. After the casting of concrete, the specimens were demoulded at the age of 2days, and the bottom surface of the beams, which was the interface between the strengthening layer and the substrate, was washed out using a retarder to obtain a roughed surface. Then the specimens were covered with wet towels for 28days in a constant temperature room (20C°). After 28days, strengthening layers were placed at the bottom side of the substrate beams. Six beams were strengthened using UHP-SHCC with the thickness of 30, 50, and 70mm (two beams for each case). And six beams were strengthened using reinforced concrete with different reinforcement ratios. Table 2 shows the type, dimensions, reinforcement and reinforcement ratios in strengthening layer, and the number of tested specimens for each case. In addition to these specimens with strengthening, two substrate beams were tested as control beams. The strengthened beams were demoulded at the age of 2days after casting of strengthening layer. The specimens were covered again with wet towels for 26days additionally.

At the age of 28days after casting of strengthening layer, loading tests were carried out by means of a four-point bending. In all tests, the lengths of the moment and shear spans were 600mm and 450mm, respectively, as shown in Fig.2. Displacements at loading points and mid point, and load were measured by displacement transducers (stroke: 50mm,

Table 1 Mix proportions of UHP-SHCC, substrate and strengthening concrete

Material	Water/ Binder*	Unit content (kg/m^3)							
		Water	Cement	Silica fume	Sand	Coarse agg.	Chemical admixture	Super-plasticizer	Fiber content (6mm)
UHP-SHCC	0.22	312.1	1342.5	237	158	---	---	31.6	14.55
Substrate & strengthening concrete	0.565	176	312	---	860	882	1.5	---	---

* Binder means cement + silica fume

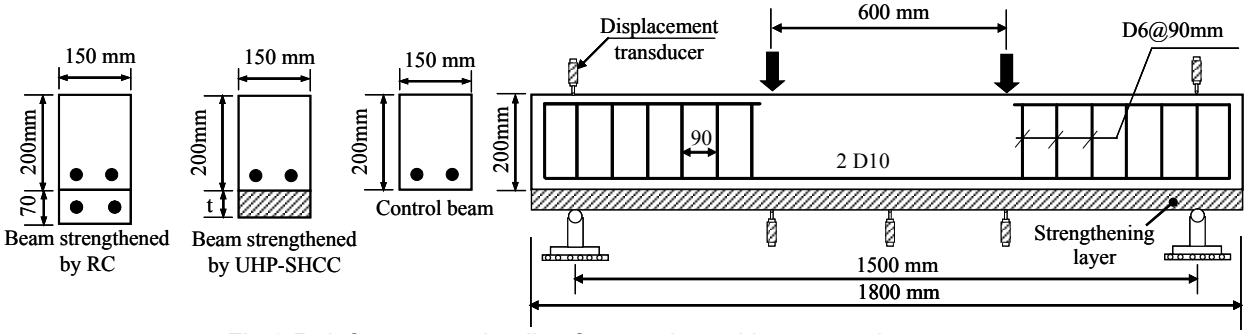

Fig.2 Reinforcement details of strengthened beams and test setup.

sensitivity: 0.005mm) and load-cell (capacity: 294kN, sensitivity: 98N), respectively. The curvature of the moment span was determined by computing the measured deflection at loading and mid points. The loading test was terminated when compressive failure of concrete on the top surface of the specimens was visually recognized or sudden drop in the load was observed.

3. EXPERIMENTAL RESULTS

3.1 Moment-curvature relation

Figs.3 and 4 show the moment-curvature curves of the beams strengthened by UHP-SHCC and RC. Table 3 tabulates obtained values on first cracking moment, yielding moment, maximum moment and curvature at maximum moment. The relation between the amount of strengthening materials (i.e. thickness of UHP-SHCC and reinforcement ratio in RC) and maximum moment are summarized in Figs. 5 and 6, respectively. In case of using UHP-SHCC as a strengthening layer, the load carrying capacity and initial stiffness of the strengthened beams were increased with increasing of the thickness of UHP-SHCC. After the localization of fracture on UHP-SHCC was observed, the moment became equal to that of the control beams, as shown in Fig.3.

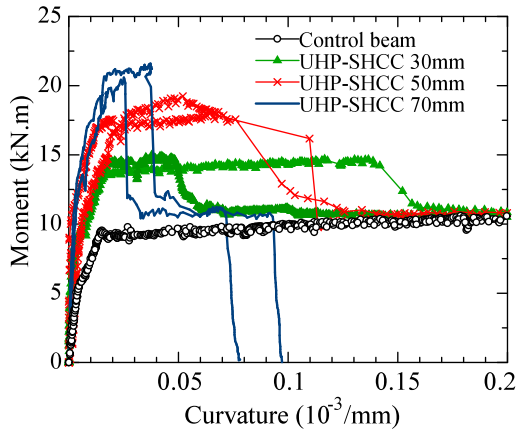

Fig.3 Moment-curvature curves of strengthened beams using UHP-SHCC

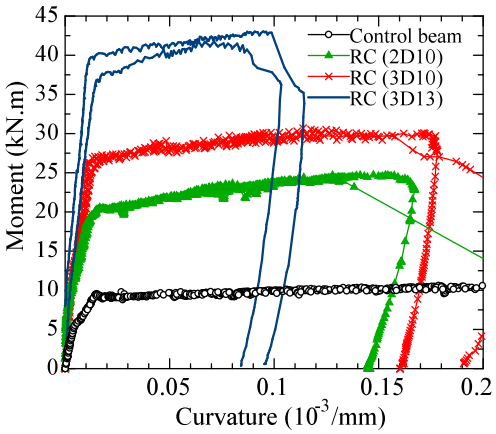

Fig.4 Moment-curvature curves of strengthened beams using RC

3.2 Crack patterns

Fig.7 shows the crack patterns of beams with UHP-SHCC (thickness: 30mm) and RC (As: 1.36%), respectively. In the specimen with RC, cracks in the strengthening layer (RC) propagated to the substrate continuously, and the number of cracks in the strengthening layer (RC) was almost the same as that of substrate. For the beams with UHP-SHCC, distributed fine cracks were observed, and the number of cracks in UHP-SHCC was dramatically increased comparing to the specimen strengthened by RC. No delamination at the interface between UHP-SHCC layer and the substrate was observed.

Table 3 First cracking, yielding, maximum moments, and curvature at maximum moment

Strengthening case		First Cracking moment (kN.m)	Yielding moment (kN.m)	Maximum moment (kN.m)	Curvature at max. moment (10^{-3}/mm)
Non. (control beam)		5.47	9.21	11.26	0.331
UHP-SHCC	t=30mm	9.02	14.00	14.84	0.077
	t=50mm	11.42	16.97	18.68	0.060
	t=70mm	11.10	20.13	21.09	0.031
Reinforced concrete (t=70mm) Reinforcement	2 D10	6.28	20.34	24.71	0.138
	3 D10	8.65	26.15	30.24	0.124
	3 D13	8.87	37.62	42.40	0.079

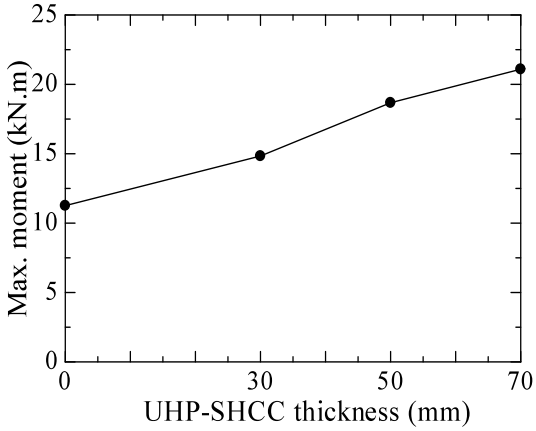

Fig.5 Effect of UHP-SHCC thickness on maximum moment

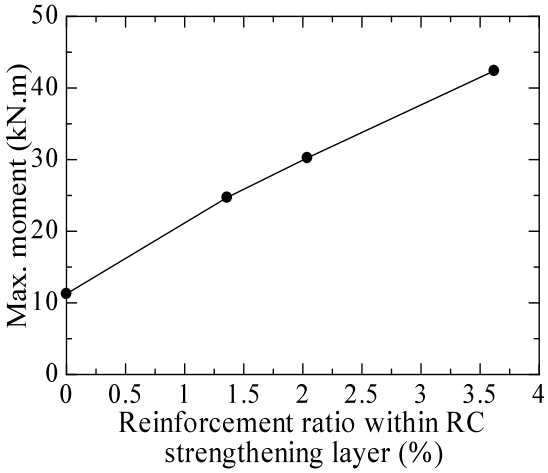

Fig.6 Effect of reinforcement ratio within RC maximum moment

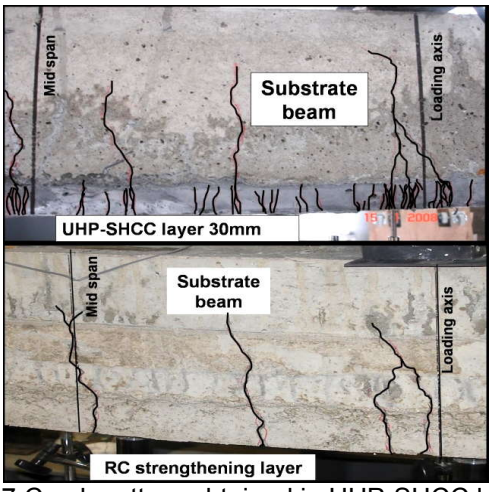

Fig.7 Crack pattern obtained in UHP-SHCC layer compared with that of RC layer

3.3 Deformation capacity and location of localized fracture of UHP-SHCC

As shown in Figs.3 and 4, the deformation capacity of the strengthened specimens that was represented by the curvature at maximum moment decreased by increasing the amount of strengthening materials, which was thickness of UHP-SHCC or reinforcement ratio in RC. The relation between the amount of strengthening materials (i.e. thickness of UHP-SHCC and reinforcement ratio in RC) and curvature at maximum moment are summarized in Figs.8 and 9, respectively.

For the specimens with RC strengthening layer, curvature at maximum moment was governed by the compressive failure of substrate concrete. However, the failure mode of the beams strengthened by UHP-SHCC depends on the fracture of the UHP-SHCC itself not on the compressive failure of the substrate concrete. In addition, in the case of using smaller thickness of UHP-SHCC (especially 30 and 50mm), tensile failure of UHP-SHCC was obtained in the moment span, as shown in Fig.10. In the case of UHP-SHCC with thickness of 70mm, that was the thickest layer in this experiment, however, the localization of fracture of UHP-SHCC was observed within the shear span not the moment span, as shown in Fig.10.

Table 4 describes the moment computed from the shear capacity of the control beam comparing to the maximum moment of the beams strengthened by UHP-SHCC. The shear capacity was calculated by the procedure specified in JSCE specification (Structural Performance Verification) [9], and the obtained moment value computed from the shear capacity was 20.07kN.m. As shown in Table 4, the maximum moment of the beam specimen strengthened by UHP-SHCC with the thickness of 70mm was similar to the moment computed from the shear capacity of the control specimen. In fact, a diagonal crack within the shear span was opened widely, as shown in Fig.10. It seems that the diagonal crack within the shear span initiated the localization of fracture on UHP-SHCC, before a tensile fracture of UHP-SHCC within the moment span.

Table 4 Comparison between the shear capacity moment of control specimen and the maximum experimental moments of UHP-SHCC specimens

Shear capacity moment of the control beam (kN.m)	Maximum experimental moment of UHP-SHCC specimens (kN.m)	
20.07	t=30mm	14.84
	t=50mm	18.68
	t=70mm	21.09

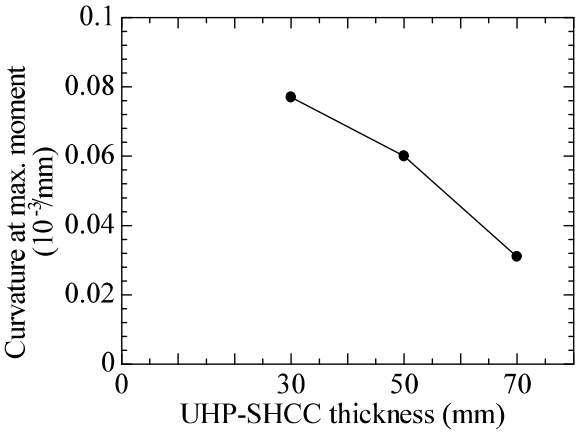

Fig.8 Effect of UHP-SHCC thickness on the deformation capacity

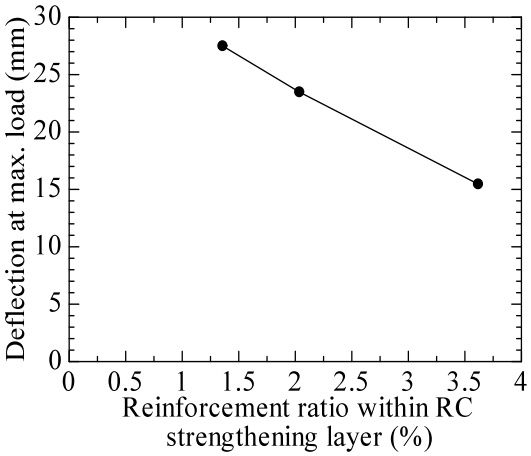

Fig.9 Effect of reinforcement ratio within the RC on the deformation capacity

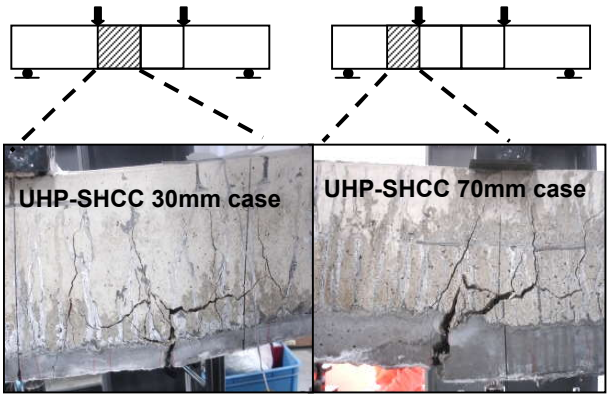

Fig.10 Effect of UHP-SHCC thickness on its failure mode

4. ANALYSIS TO PREDICT RESPONSE OF BEAM

4.1 Analysis flow

Moment-curvature analysis was carried out to predict moment-curvature relations for the beams strengthened by UHP-SHCC. The analysis depended on the assumption that "plane sections remain plane". Analysis flow is as follows:

- The input data include the specimen size, and stress strain relationships of the concrete, UHP-SHCC, and reinforcement.
- Give the strain at extreme compression fiber as the increment parameter.
- Compute the stress corresponding to the strain at each fiber level (according to stress-strain relationships of the materials).
- Determine the depth of the neutral axis that causes the equilibrium.
- Compute the moment and curvature at equilibrium stage, and then repeat the same procedure after giving new strain increment.
- The analysis was terminated if any of these cases happened: compression failure of the ordinary concrete, or tension failure of UHP-SHCC.

4.2 Materials models

About the stress-strain relationships of the materials used in analysis:

(1) UHP-SHCC: From the stress-strain curves of UHP-SHCC in uniaxial tensile test, using the averaged first cracking stresses and averaged maximum tensile strengths and corresponding strains, the averaged stress-strain curve, shown in Fig.1, was used for the material response of UHP-SHCC in tension.

(2) Ordinary concrete: Fig.11 illustrates the compressive stress-strain relationship of the ordinary concrete for the substrate used in the analysis. The concrete stress value was governed by Eq.1 up to strain value equal to 0.002. The stress value after the strain exceeds 0.002 is equal to 85% of compressive strength of the concrete (f'_c=24MPa). When the strain value of concrete exceeded 0.0035, the analysis was terminated. The material response in tension of the ordinary concrete was neglected in the analysis.

$$\sigma_c = \begin{cases} k_1 f_c' \times \dfrac{\varepsilon_c}{0.002} \times \left(2 - \dfrac{\varepsilon_c}{0.002}\right) & \varepsilon_c \le 0.002 \\ k_1 f_c' & \varepsilon_c > 0.002 \end{cases} \quad (1)$$

where,

σ_c : compression stress of concrete
f_c' : compressive strength of concrete
ε_c : compression strain of concrete
$k_1 = 1 - 0.003 f_c' \le 0.85$

(3) Reinforcement: Fig.12 shows tensile stress-strain relationship of the reinforcement used in the analysis. Bilinear stress-strain relationship was used in the analysis, as described in Fig.12 and Eq.2.

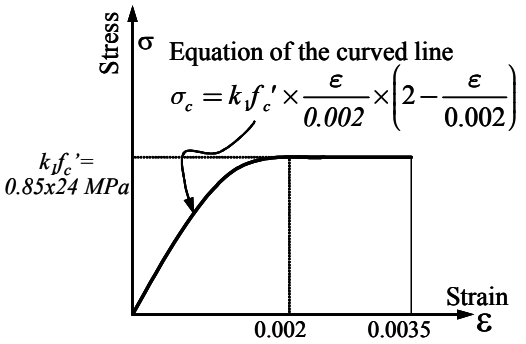

Fig.11 Compressive stress-strain curve of ordinary concrete used in moment curvature analysis

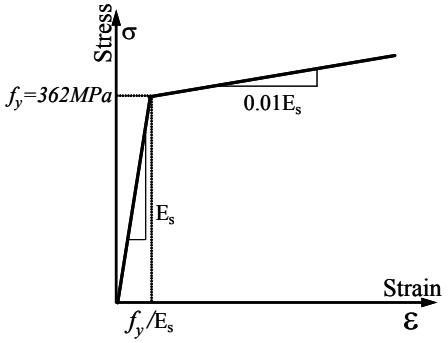

Fig.12 Tensile stress-strain curve of the reinforcement used in moment curvature analysis

$$\sigma_s = \begin{cases} \varepsilon_s . E_s & \varepsilon_s \le f_y / E_s \\ f_y + 0.01 E_s . (\varepsilon_s - f_y / E_s) & \varepsilon_s > f_y / E_s \end{cases} \quad (2)$$

where,

σ_s : tensile stress of reinforcement
E_s : Young's modulus of reinforcement
ε_s : tensile strain of reinforcement
f_y : yield strength of reinforcement

Fig.13 shows a comparison between the moment-curvature curves obtained from the analysis and experiment for the beams strengthened by UHP-SHCC. In case of beams with UHP-SHCC having the thickness of 30mm, the analysis showed that tensile failure of UHP-SHCC was obtained before the compressive failure of substrate concrete, and this behavior was well agreed with the experimental failure mechanism. In the cases of 50 and 70mm thickness, the analysis showed that the compressive failure in concrete was occurred before the failure of UHP-SHCC. The comparison showed good agreement between experimental and analytical results up to reinforcement yielding point in all cases, as shown in Fig.13. For beams with 70mm thickness of UHP-SHCC, the difference between the analytical and experimental curves increases rapidly after the yielding point. As mentioned before, a major diagonal crack in shear span was observed in the experiment, and the crack might initiate the (shear) failure of UHP-SHCC, before tensile failure of UHP-SHCC itself.

Generally, the experimental results of beams with UHP-SHCC can be roughly simulated by the

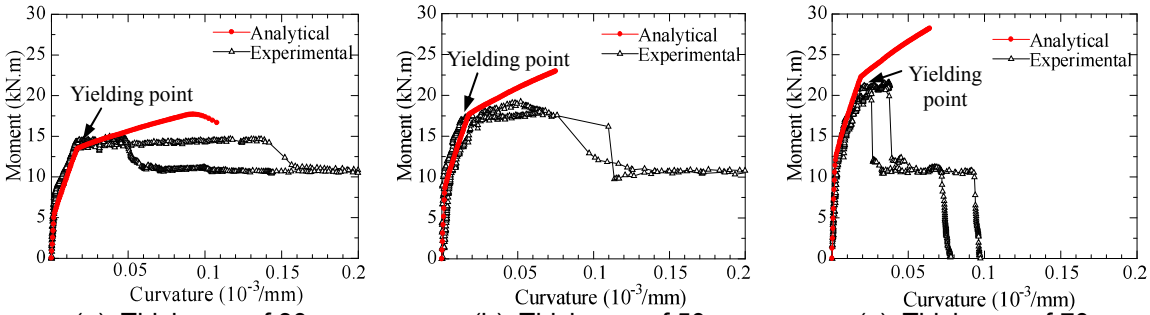

(a): Thickness of 30mm (b): Thickness of 50mm (c): Thickness of 70mm

Fig.13 Comparison between analytical and experimental moment-curvature curves of beams strengthened by UHP-SHCC

analysis using the above material response, except for the beams with UHP-SHCC having the thickness of 70mm. From this analysis and study, it was revealed that the material response of UHP-SHCC obtained from the tensile tests can be used to predict the response of strengthened beams, except for the deformation capacity of beams with thicker UHP-SHCC (70mm in this study).

5. CONCLUSIONS

In order to discuss the strengthening effect of RC beams with UHP-SHCC, four-point bending tests were carried out, in addition to the analysis to predict moment-curvature relations. The following conclusions were obtained:

(1) The load carrying capacity and initial stiffness of the strengthened beams were increased with increasing of the thickness of UHP-SHCC.
(2) For the beams with UHP-SHCC, distributed fine cracks were observed, and the number of cracks in UHP-SHCC was dramatically increased comparing to the specimen strengthened by RC. In addition, no delamination at the interface between UHP-SHCC layer and the substrate was observed.
(3) The failure mode of the beams strengthened by UHP-SHCC depends on the localized fracture of the UHP-SHCC itself not on the compressive failure of the substrate concrete. In the case of using smaller thickness of UHP-SHCC (especially 30, and 50mm), tensile fracture of UHP-SHCC was obtained in the moment span.
(4) The localized fracture of UHP-SHCC was observed within the shear span not the moment span in the case of UHP-SHCC with thickness of 70mm. It seems that the diagonal crack within the shear span initiated the localization of fracture on UHP-SHCC, before a tensile fracture of UHP-SHCC within the moment span.
(5) The experimental results of beams with UHP-SHCC can be roughly simulated by the analysis using the material response obtained from the tensile test.

ACKNOWLEDGEMENT

This research was financially supported by Service Center of Port Engineering (SCOPE). The fibers were provided by Toyobo Co., Ltd, and chemical admixture was provided by Takemoto oil&fat Co., Ltd. The authors would like to thank those supports.

REFERENCES

[1] T. Kanda, S. Watanabe, and V.C. Li: Application of Pseudo Strain Hardening Cementitious Composites to Shear Resistant Structural Elements, Fracture Mechanics of Concrete Structures, FRAMCOS-3 Proceedings, pp.1477-1490, Oct. 1998
[2] H. Fukuyama, Y. Sato, V. C. Li, Y. Matsuzaki, and H. Mihashi: Ductile Engineered Cementitious Composite Elements for Seismic Structural Applications, 12th WCEE Proceedings, 2000.
[3] J. Zhang, C.K.Y. Leung, and Y. Cheung: Flexural performance of layered ECC-concrete composite beam, Journal of Composites Science and Technology, Vol. 66, pp1501–1512, 2006.
[4] H. Horii, S. Matsuoka, P. Kabele, S. Takeuchi, V.C. Li, and T. Kanda: On the Prediction Method for the Structural Performance of Repaired/Retrofitted Structures, Fracture Mechanics of Concrete Structures, FRAMCOS-3 Proceedings, pp.1739-1750, Oct. 1998.
[5] V.C. Li: ECC for Repair and Retrofit in Concrete Structures, Fracture Mechanics of Concrete Structures, FRAMCOS-3 Proceedings, pp. 1715-1726, Oct. 1998.
[6] V.C. Li, H. Horii, P. Kabele, T. Kanda, and Y.M. Lim: Repair and Retrofit with Engineered Cementitious Composites, International Journal of Engineering Fracture Mechanics, Vol.65, No.2-3, pp.317-334, 2000.
[7] S.K. Shin, J.J.H. Kim, Y.M. Lim: Investigation of the strengthening effect of DFRCC applied to plain concrete beams, Journal of Cement & Concrete Composites, Vol. 29, Issue 6, pp. 465-473, 2007.
[8] M. Kunieda, E. Denarié, E. Brühwiler, H. Nakamura: Challenges for Strain Hardening Cementitious Composites – Deformability Versus Matrix Density, Proc. of the fifth International RILEM Workshop on HPFRCC, pp.31-38, 2007.
[9] Standard Specifications for Concrete Structures, Structural Performance Verification, JSCE Guidelines for Concrete No.3, pp.76-78, 2002.